TISSUE ENGINEERING: Part C
Volume 18, Number 3, 2012

DOI: 10.1089/ten.tec.2011.0233

Design and Validation of a Compressive Tissue Stimulator with High-Throughput Capacity and Real-Time Modulus Measurement Capability

David J. Salvetti, B.E.,[1,*] Christopher J. Pino, Ph.D.,[1,*] Steven G. Manuel, M.S.,[2] Ian Dallmeyer, M.E.,[1] Sanjeet V. Rangarajan, M.D., M.E.,[1] Tobias Meyer, M.E.,[1] Misha Kotov, B.E.,[3] and V. Prasad Shastri, Ph.D.[1,4]

Mechanical stimulation has been shown to impact the properties of engineered hyaline cartilage constructs and is relevant for engineering of cartilage and osteochondral tissues. Most mechanical stimulators developed to date emphasize precision over adaptability to standard tissue culture equipment and protocols. The realization of mechanical characteristics in engineered constructs approaching native cartilage requires the optimization of complex variables (type of stimulus, regimen, and bimolecular signals). We have proposed and validated a stimulator design that focuses on high construct capacity, compatibility with tissue culture plastic ware, and regimen adaptability to maximize throughput. This design utilizes thin force sensors in lieu of a load cell and a linear encoder to verify position. The implementation of an individual force sensor for each sample enables the measurement of Young's modulus while stimulating the sample. Removable and interchangeable Teflon plungers mounted using neodymium magnets contact each sample. Variations in plunger height and design can vary the strain and force type on individual samples. This allows for the evaluation of a myriad of culture conditions and regimens simultaneously. The system was validated using contact accuracy, and Young's modulus measurements range as key parameters. Contact accuracy for the system was excellent within 1.16% error of the construct height in comparison to measurements made with a micrometer. Biomaterials ranging from bioceramics (cancellous bone, 123 MPa) to soft gels (1% agarose, 20 KPa) can be measured without any modification to the device. The accuracy of measurements in conjunction with the wide range of moduli tested demonstrate the unique characteristics of the device and the feasibility of using this device in mapping real-time changes to Young's modulus of tissue constructs (cartilage, bone) through the developmental phases in *ex vivo* culture conditions.

Introduction

It is well established that mechanical stimulation improves the mechanical properties of engineered cartilage constructs grown *ex vivo* from dissociated cells. Along with biological signals,[1,2] mechanical stimuli are important in the optimization of the mechanical properties and biochemical composition of engineered cartilage.[3] Several studies have shown that the application of direct compressive, hydrostatic, and shear forces improves the biosynthesis of extra cellular matrix components and increases the macroscopic material properties of engineered cartilage.[4–6] Additionally, it has been shown that dynamic compression can enhance the uptake of biological signals within cartilage constructs.[7] With regard to engineering hyaline cartilage constructs with appropriate weight-bearing characteristics, mechanical stimulation remains one of the most promising approaches.[4,6,8] The realization of functional *ex vivo* constructs through mechanical stimulation will require the optimization of regimen variables including magnitude and type of stress, frequency, duty cycle, duration of stimulation regimen, mass transport considerations, and cell culture environment (growth factors, oxygen tension).[8,9] Furthermore, optimal functional outcomes in engineered hyaline cartilage and osteochondral constructs may require the application of a complex stimulation regimen comprised of a combination of compressive, shear, or hydrostatic forces with simultaneous exogenous signals. Due to the large number of possible variables required to optimize stimulation regimens, we have concluded that high-throughput is the most important

Departments of [1]Biomedical Engineering, [2]Mechanical Engineering, and [3]Electrical Engineering, Vanderbilt University, Nashville, Tennessee.
[4]Institute for Macromolecular Chemistry and BIOSS Center for Biological Signalling Studies, University of Freiburg, Freiburg, Germany.
*These two authors equally contributed to this work.

design criterion for a mechanical stimulator. We define high-throughput as the capability to configure a device to test the maximum number of variables with minimal time requirements for device reconfiguration.

Direct compression mechanical stimulators for cartilage developed to date[10–12] emphasize precision while not adequately addressing throughput and adaptability to the everyday tissue culture environment. For instance, typical bioreactor designs seldom incorporate the ability to apply multiple stress types.[13] In order for mechanical properties of engineered constructs to be measured, two separate devices, a stimulator unit and separate mechanical testing unit, are required many times.[12] Transferring samples between devices consume time and become an additional opportunity for contamination. Of current designs, the proprietary nature of the stimulator components, such as construct trays, construct plungers, and load cells, requires machining of new parts to accommodate changes to construct number and size.[10,11] A stimulator design recently reported by Lujan *et al.* has taken into consideration the adaptability to standard disposable tissue culture trays and demonstrated the capability to measure force on individual samples through the use of dedicated electromagnetic actuators.[14] However, due to the size of the electromagnetic actuators, they are limited to a six-well plate. This shortcoming restricts stimulation and constructs evaluation throughput.

Many manufacturing and usability issues, along with cost, are significant factors impeding the widespread implementation of existing stimulation device designs for tissue engineering applications. Our stimulator design, therefore, focused on high construct capacity, regimen adaptability, and broad operating parameters to include specimens of varying Young's moduli (herein referred to as modulus), all while minimizing stimulator cost. Herein, we propose the design of a direct compression stimulator which is compatible with standard tissue culture multi-well formats, and that functions inside a standard CO_2 incubator. It is amenable to high-throughput experimentation while maintaining the requisite precision for cartilage stimulation. As depicted in Figure 1, the design uses commercially available off-the-shelf components, and easily machined aluminum parts, which can be implemented for under $4000. The modular design should enable the device to be reconfigured for several stimulation protocols in a short time with minimum expense. Adaptability and throughput limitations were overcome by using small variable resistor force sensors, which individually address constructs in each construct well. The force transmitted through individual constructs is, therefore, recorded in real time, enhancing the stimulator's ability to measure Young's modulus during experimentation. This is a novel element of this stimulator design and represents a significant improvement over past designs.

Materials and Methods

Mechanical components

Figure 1 schematically depicts the physical design of the device. There are several noteworthy mechanical design

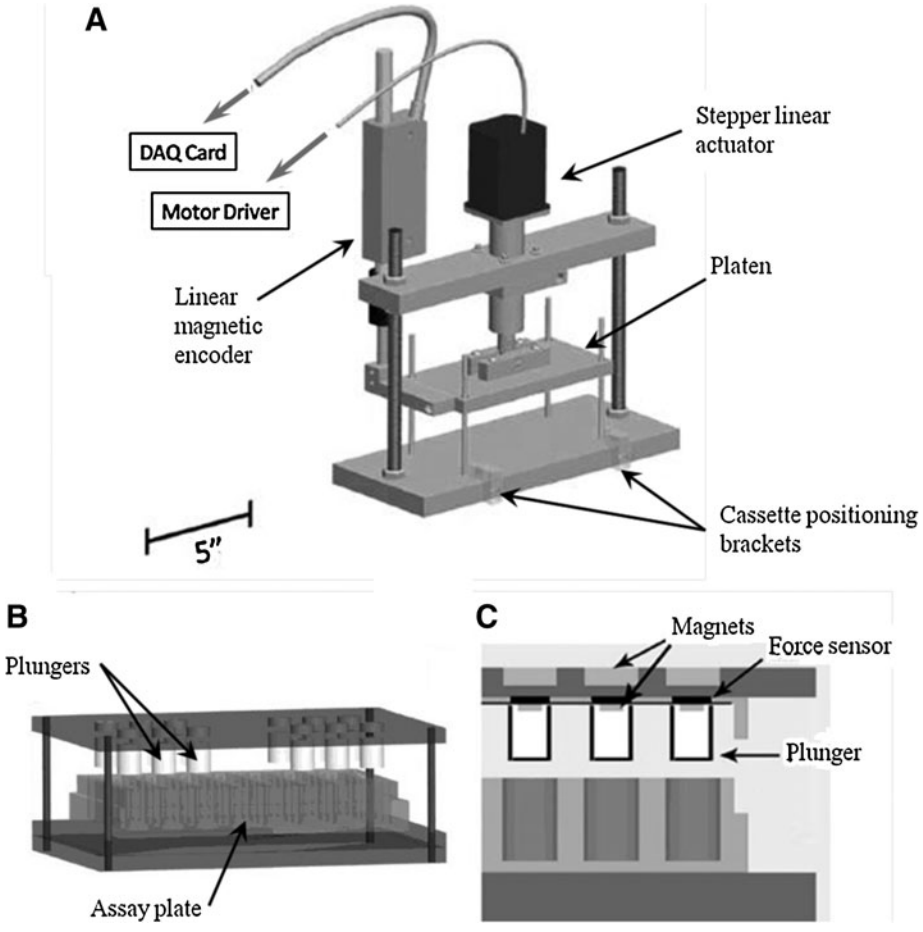

FIG. 1. **(A)** Design of the mechanical stimulator without the stimulation cassette in place **(B)** Stimulation cassette with tissue culture plastic snapped in place and Teflon plungers attached to upper magnets **(C)** Cross section of stimulation cassette depicting alignment of plungers with plastic wells and magnet attachment.

elements. All metal components are machined out of aluminum, an easily and inexpensively machined metal. The platen travels along guide rods via four plastic sleeve bearings to prevent jamming. An Ultramotion D-B.125-HT23-2-/RC4 linear actuator is attached via a tube clamp to the upper cross brace. It attaches to the platen via a bolt through a machined block that matches the dimensions of the shaft. The motor moves in 5 μm increments and is accurate to 10 μm. A Newall Electronics absolute linear encoder model SPB-TS is utilized to obtain the position of the platen. It attaches to the upper cross brace using a highly rigid machined L-bracket. The encoder scale attaches to the platen with another custom bracket and since the encoder is highly sensitive to perturbation, a steel braid attachment from the manufacturer is included to allow for minor radial misalignment and vibration without damaging the encoder. The overall size is $30 \times 12 \times 34$ cm and will fit inside a standard CO_2 incubator.

One of the several design elements that promotes high throughput and adaptability is the removable Lexan® polycarbonate stimulation cassette. Figure 1b, c depict the cassette alone, while Figure 1a depicts the stimulator loaded with the cassette. Similar to the platen, the upper portion of the cassette is guided by bronze guide rods allowing vertical movement. A rectangular channel is machined into the surface of the lower portion of the cassette to allow standard plastic assay wells to *snap-fit* into the base. The upper cassette plate is elevated from the construct plate by four light coil springs. In the configuration tested, 12 neodymium magnets are pressed into milled holes in the top surface of the upper plate. The magnets are arranged to align with wells in a 48-well assay plate. Twelve cylindrical Teflon® plugs with correspondingly smaller neodymium magnets pressed into their upper surface are suspended from the bottom of the upper cassette plate. The Teflon plugs mechanically contact the cartilage constructs (See the inset of Figure 1c for a cross section of the cassette construction). The plugs measure 8.3 mm in diameter, while the wells of a 48-well plate are 10 mm in diameter allowing room for cell media to displace.

Sandwiched between the plugs and the upper cassette plate is a force sensor network. Twelve Tekscan Inc. FlexiForce model A210 sensors were arranged so that each Teflon plug pushes against a single force sensor. The sensors are laminated between two thin adhesive-backed polyethylene terephthalate (PET) sheets to maintain their orientation and position.

Device electronics and software

Figure 2 details the connection diagram and feedback diagram of the external control box constructed using an IEEE approved desktop computer enclosure. The box contains an Anaheim Automation stepper motor driver, a National Instruments data acquisition (DAQ) device model 6210, two switching power supplies, and a proprietary circuit board of 12 amplifier circuits. Controlling the device requires a number of input and output signals. These signals are either created or analyzed using a custom software package created in National Instruments LabView 8.5. Using subroutines in the software, the motor driver is controlled by a clock, direction, and power signal. The linear encoder is interpreted through two counter inputs of the DAQ card and another subroutine. The 12 force sensors are wired to the custom circuit board mounted inside the box. On the board, each

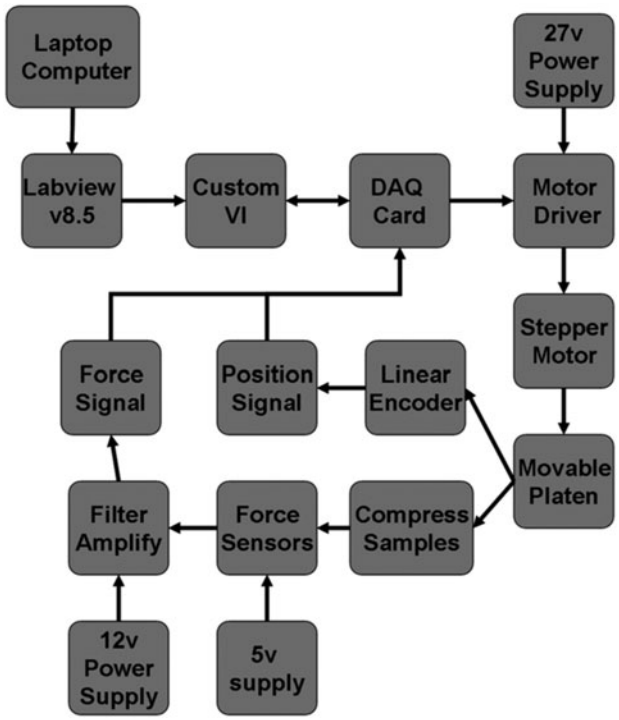

FIG. 2. Schematic of the control loop of the mechanical stimulator.

sensor uses a current to voltage converter consisting of an inverting op-amp circuit. The feedback resistor of the op-amp circuit has a value of 499 ohms. This resistor determines both the range and sensitivity of the force sensors. Decreasing the resistance decreases the sensitivity and the increases range. 10 μf capacitors were added to the inverting op-amp configurations to act as low-pass filters. The output of the amplifiers is connected to the DAQ card for capture and interpretation by the software. Both the position data from the linear encoder and the voltage outputs from the force sensors are saved with time stamps for data analysis. From this data, calculations may be performed to extract modulus values, differential construct heights, order of construct contact, strain rates, and so on.

The control loop for stimulation functions in the following manner. The motor initially pushes the platen in the downward direction while monitoring information from the force sensors. Once all sensors register a threshold voltage as defined by the user, the position of the device from the linear encoder is stored as a reference position. The stimulation routine is then implemented. The motor continues to push downward until the desired stimulation distance (also adjustable by the user) is achieved. The direction of the motor is then reversed until it reaches the reference position where it again reverses direction. The device is currently configured to stimulate with a triangular displacement waveform, but can be easily adapted to more complex waveforms. This loop operates continually until the device is stopped.

Force sensor calibration

The individual sensors in the force sensor network required calibration to correlate output voltage to force. To

eliminate the possibility of the magnetic field of the plunger attachment system altering sensor readings, the calibration was performed with the force sensor network sandwiched between magnets to simulate usage. This was accomplished by removing the sensor network and the top of the removable cassette and placing them flat and upside down on a bench top. In order to ensure the balanced placement of calibration weights, a shortened plunger-magnet assembly was placed on top of the sensor with the vertical axis perpendicular to the sensor face, and ASTM Class 1 weights ranging from 5 to 500 g were placed on the face of the plunger. Calibration curves relating force and output voltage were recorded. A linear regression was performed on the data from each sensor giving a mathematical model for the force applied. From the calibration, the force range and resolution of the sensors were determined, as well as a coefficient for each sensor (C_{sensor}) to relate voltage to force. The minimum detectable force was determined by the y-intercept of the linear regression performed on the force-voltage data. The maximum detectable force was calculated for an output of 9 V. This value was chosen to be slightly lower than the rails of the op-amps to avoid nonlinear amplifier behavior. The resolution of each sensor was calculated based on the minimum detectable voltage change in our system, 0.01 V.

Position measurement error determination

The error associated with position measurements was established by running the motor for an arbitrary amount of time and measuring the displacement of the platen using a dial caliper ($n=10$). These values were compared with the displacement recorded by the linear encoder.

Simultaneous construct height measurement

Ten compressible silicone (Silastic) constructs of varying heights were used for this portion of the evaluation. The height (h) of the construct was accurately determined using a friction type micrometer (Mitutoyo). The difference between the smallest and largest construct used in this study was 0.93 mm. Silastic was chosen due to similar compressible properties as cartilage. The 10 constructs were then loaded into a 48-well plate and compressed with the device. Two wells were left blank to act as negative controls. Data was collected for the 10 constructs simultaneously. Using the tallest silicone construct as a zero point, construct heights were extracted from the saved data. The construct heights measured using the device were compared with those measured using a micrometer.

Real-time modulus measurements

Modulus was calculated through the analysis of stress-stain data as it was acquired. The first contact of a stimulator plunger and a construct was defined as a 0.4 V signal. This value was chosen, as it represents a signal value greater than the maximum noise for the sensor array. All voltage measurements from the device were converted into force (N) (Eq. 1), where C_{Sensor} is a calibrated coefficient for each sensor, and stress (Pa) is calculated (Eq. 2), using an assumed constant construct area (m^2). Linear displacement data (m) was converted into strain using the measured construct height (m) (Eq. 3). To avoid aberrant nonlinear behavior at low or high stress values, the modulus was calculated at varying strains appropriate for the material. For instance, hard, brittle materials such as cancellous bone required modulus measurements at low strain values (<1%). Supplementary Figure S1 (Supplementary Data are available online at www.liebertonline.com/tec) illustrates the raw data during the compression of cartilage samples and depicts the initial nonlinear region and the area where modulus is calculated (Supplementary Fig. S1).

$$\text{Force} = C_{sensor} \times \text{Voltage} \quad \text{(Eq. 1)}$$

$$\text{Stress} = \text{Force}/\text{Area}_{construct} \quad \text{(Eq. 2)}$$

$$\text{Strain} = \text{Displacement}_{\text{Linear Encoder}}/\text{Height}_{construct} \quad \text{(Eq. 3)}$$

$$\text{Modulus} = \text{Stress}/\text{Strain} \quad \text{(Eq. 4)}$$

Modulus measurement verification

A key function of the stimulator design is to track changes in modulus of stimulated constructs over time. This capability to detect modulus differences was verified by measuring the modulus of four different materials of varying degrees of stiffness, ranging from hydrogels to biological specimens.

Agarose gels. Wells ($n=12$ for each w/v% agarose) of a 48-well plate were loaded with high melting agarose hydrogel ranging in concentration from 1–8 w/v% incremented in 1% intervals. Each well plate was then loaded using the device, and the modulus of the material was calculated using a linear regression on the stress strain data.

Alginate gels. In addition to agarose gels, alginate gels formed by ionic crosslinking of Alginic acid with calcium ions were also studied. Since above 75 mmol, the concentration of $CaCl_2$ has been shown to make no difference in the modulus of the material,[15] gels were prepared using 100 mmol $CaCl_2$. The modulus of 2%, 3%, and 4% alginate gels was measured and compared with published values ($n=12$ for each concentration).

Porcine cartilage and cancellous bone. Since one of the intended applications of the stimulator is cartilage and bone stimulation, porcine cartilage and cancellous bone were also tested. The cartilage was harvested from freshly euthanized mini pigs by lateral dissection of the joint through the synovial capsule to expose the joint space. The menisci were then removed to expose the articular surfaces of the femur and tibia. Using a cork-borer (diameter = 7 mm), 18 articular osteochondral plugs were cored out and transferred into 50 mL centrifuge tubes containing sterile Dulbecco's modified Eagle's media (Mediatech, Inc.) supplemented with 10% fetal bovine serum (HyClone) and penicillin/streptomycin (Mediatech, Inc.). The cartilage portion of the explants was carefully dissected from the underlying cancellous bone while maintaining the integrity of the underlying cancellous bone. The explants (constructs) were then sliced to uniform thickness for modulus measurements. The cartilage explants ($n=9$) were then immediately transferred to the stimulator tray, and the modulus of the constructs was measured. Each plug was tested thrice with a 10 min interval between runs to allow the cartilage to equilibrate. The modulus values were then compared with known values from literature. Similarly,

cancellous bone specimens were prepared and tested, and their moduli were compared with values reported in the literature.

Digested cartilage constructs. Since one of the unique design features of this stimulation device is the ability to simultaneously detect changes to specimen modulus, one can envisage that the changes in ECM composition of an engineered cartilage can be followed in real time. Since collagen is key for ensuring compliance in cartilage, to explore this aspect of the device, the modulus of 9 cartilage constructs depleted of collagen was also tested. Collagen depletion was achieved by subjecting the constructs to enzymatic digestion using a 0.2% type II collagenase (C1764; Sigma-Aldrich) for 12 h, as it has been shown that full digestion will occur at this concentration between 12 and 16 h.[16] Digested constructs were cultured in the collagenase solution ($n=9$) in a humidified cell culture incubator at 37°C and 5.0% CO_2 for 12 h.

Histological sectioning and staining of cartilage

Control and collagenase digested constructs were fixed overnight in formalin, and embedded in paraffin after dehydration using an ethanol series (50%, 70%, 80%, 90%, and 100%), followed by xylene substitution. Using a cryomicrotome, 10 μm-thick transverse sections were cut and stained with Hematoxylin and Eosin to reveal cell nuclei and connective tissue, and Safranin O was counterstained with fast green to visualize proteoglycans.

Culture environment reliability testing

As a part of the device design, components were selected to be compatible with a tissue incubator environment. To ensure device reliability was not affected by humidity and temperature, the stimulator was placed in a cell incubator with a 5% CO_2 and 100% humidity atmosphere. The ability of the stimulator to execute a compression regimen over 36 h was tested to identify whether malfunctions would occur under these conditions.

Results

Mechanical stimulation

The ability to impose stimulation regimens at various frequencies was verified using 8% agarose plugs. Figure 3 shows a stimulation regimen of 5% dynamic strain superimposed on a 5% static load at four different frequencies (0.090, 0.175, 0.900, and 1.450 Hz) over a 10-s period.

Force sensor calibration

The stimulator design described enables the concurrent measurement of modulus during the stimulation protocol. To enable this, force sensors were implemented in between the plunger and the cover of the stimulation cassette (Fig. 1C). The force sensors were calibrated to determine the correlation coefficient between the output voltage from the sensor and force (N). The highest and lowest slope calibration curves, along with the average calibration curve and standard deviations for the 12 sensors, are shown in Figure 4. The average minimum detectable force per sensor was 189 mN. This corresponds to 0.2% compression of an 8% agarose plug assuming a Young's modulus value of 664.2 kPa (see Fig. 5). The average resolution was 12 mN, and the average maximum detectable force per sensor was 10.7 N, which corresponds to 10.5% compression of an 8% agarose plug. The sensor calibration data displays the high sensitivity of the resistive sensors, which enable accurate, reproducible measurements.

Position and construct height measurement

A key criteria in past stimulator designs has been accurate position measurement. The average absolute position error of the linear encoder was found to be 1.66% ± 0.96%, which was the deviation between construct heights as measured by the linear encoder versus the actual height of the construct as measured by a micrometer. Data for Silastic construct height measurements are presented in Table 1. For a simultaneous measurement of 8 Silastic construct mimics varying in height by a maximum of 0.93 mm, the average absolute construct height measurement error was found to be 1.16% ± 0.93%, with a maximum error of 2.91%. The accuracy of measurement is comparable to past designs[11] with the added capability of simultaneous construct height characterization.

Modulus of hydrogels derived from natural polymers: agarose and alginate

In mechanical tissue stimulation, it is critical for the measurement device to be capable of measuring the modulus of materials accurately over a wide range of material properties. In order to demonstrate the accuracy of modulus measurements made with the mechanical stimulator, elastic modulus of well-characterized materials, agarose,[12] and alginate gels,[15] were measured as a function of concentration (w/v). Modulus measurements for increasing concentrations of both agarose and alginate gels are shown (Fig. 5, Table 2), and were statistically similar to previously published studies.[12,15] A typical curve of the sensor voltage as a function of time from the compression of a cartilage construct is shown in Supplementary Figure S1.

Young's modulus of biological tissues, cartilage, and cancellous bone

In order to validate the utility of this device in the determination of modulus of biological materials, cartilage, digested cartilage, and cancellous bone were loaded, and modulus measurements were acquired (Table 2). Young's modulus measurements of normal porcine articular cartilage from the distal head of the femur (3.4 ± 0.6 MPa) were not statistically different than previously published values (2.6 ± 0.1 MPa).[17] Cartilage treated with collagenase for 12 h exhibited a significantly lower measured modulus (1.5 ± 0.2 MPa) than native cartilage. Histology further confirmed that the digestion of cartilage with collagenase leads to depletion of type-2 collagen and the loss of proteoglycan content as shown in Figure 6B, D. The highest modulus biological tissue tested, cancellous bone, had a measured average modulus of 123 MPa, with a standard deviation of 27 MPa, which is within the range previously published by Cowin *et al.*[18] Modulus for cancellous bone, which is a porous material, was calculated using MacKenzie's Equation,[19]

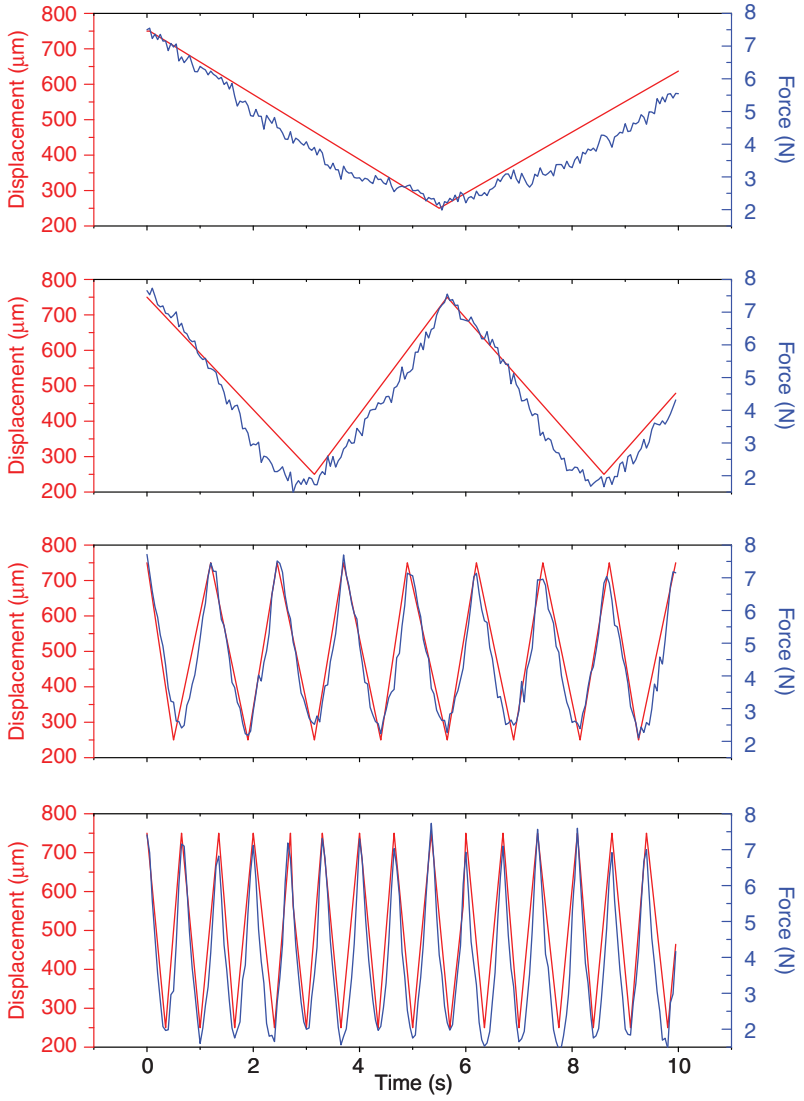

FIG. 3. Displacement and force measurements from cyclic stimulation of silicone constructs at four different frequencies. From top to bottom: 0.090, 0.175, 0.900, and 1.450 Hz. Silicone was chosen for possessing similar elastic properties to cartilage. Color images available online at www.liebertonline.com/tec

a well-established correlation of measured apparent modulus and porosity (Eq. 5), with an assumed porosity of 20% or a void space of 80%, which is a conservative, average estimate for cancellous bone beneath the articular cartilage of the distal femur head.[18]

$$E = E_{\text{apparent}}/(1 - (1.9 \times \text{Porosity}) + (0.9 \times (\text{Porosity}^2))) \quad \text{(Eq. 5)}$$

Culture environment reliability testing

After 36 h in a cell incubator, the stimulator responded to the prescribed compression cycle without faults or failures during the test. Based on this, we conclude that the stimulator is suitable for long-term use in the environment of a tissue incubator.

Discussion

Real-time measurements of modulus of biomaterials ranging from soft polymers (1% agarose gels; $E = \sim 20$ KPa) to a hard bioceramic (porcine cancellous bone; $E = \sim 120$ MPa) were enabled by the unique design of this mechanical stimulator. In addition to the wide dynamic range of modulus, the design device shows high sensitivity to changes in material composition, such as changes in extracellular matrix composition in cartilage. These results taken together verify that the stimulator is capable of sensitive and accurate mechanical measurements in a range which includes the mechanical properties of acellular cartilage constructs, seeded constructs during *ex vivo* culture, and constructs approaching the properties of biological tissues, with a high maximum modulus measurement capability.

Design comparison

An image of the completely assembled and functional device is shown in Supplementary Figure S2. The proposed design excels in three key areas: *individual force sensing*, *throughput*, and *cost*. Table 3 compares key operating parameters and features of the proposed design to three published designs[10,11] highlighting differences in specifications.

The advantages of implementing individual construct force sensors are numerous. The sensors allow for the determination of modulus concurrently with stimulation. This

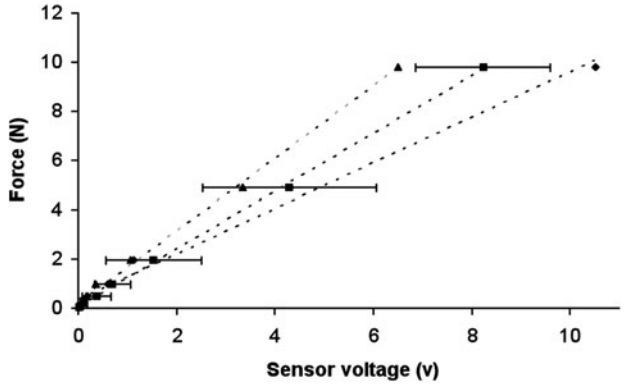

FIG. 4. Calibration of force sensors showing the correlation of measured voltage and applied force. The values shown are the average of all force sensors ± 1 standard deviation (squares) and the extreme force sensors: the sensor with the highest force calibration coefficient (triangles), and the lowest (diamonds).

Table 1. Precision of Simultaneous Measurement of Silicone Plug Samples of Varying Height

Measured by micrometer (mm)	*Measured by stimulator (mm)*	*% Difference*
10.06	9.94 ± 0.01	1.23
9.95	9.95 ± 0.01	− 0.03
9.76	9.75 ± 0.03	− 0.15
9.54	9.62 ± 0.02	− 1.14
9.53	9.48 ± 0.01	0.53
9.40	9.53 ± 0.03	− 1.80
9.38	9.45 ± 0.03	− 0.57
9.27	9.51 ± 0.02	− 2.91
9.15	9.37 ± 0.01	− 2.29
9.13	9.20 ± 0.02	− 0.99

increases the *throughput* of the device by enabling continuous data acquisition, and, therefore, increases temporal resolution for evaluating time-dependent stimulation regimes. Furthermore, *in situ* modulus measurement reduces loss in productivity associated with transferring constructs to a separate mechanical tester at prescribed time points and possible sample contamination. Besides throughput, individual sensors enable the height of constructs to be simultaneously measured. This bestows the user with two options to avoid lift off from shorter samples. First, plungers of different heights may be substituted such that contact is achieved on all samples at the same time. This capability is unique to our device, as many designs utilize fixed plunger systems. Second, static offset strain may be increased to a higher value than the height variation of samples. Biological constructs are inherently variable, and, therefore, this capability ensures each construct is subjected to the prescribed displacement. Albeit, large variations in sample height will alter the intended strain, for instance, imposing a 100 μm displacement on a 2 mm thick sample imposes a 5% strain, while a 1.5 mm thick sample would experience a 6.6% strain. The strain variation is reduced with more typical 4–5 mm thick samples. Finally, individual force sensors and actuators allow for discrete stimulation and material property measurement from individual constructs in separate compartments. This enables the use of standard tissue culture plastic well-plate formats to culture individual constructs in different environments with various biomolecular regimens to increase experimental throughput.

The only other device with individual sensing is the Lujan design.[14] Their device functions by prescribing a force and measuring the displacement experienced by a sample. This requires the user to have previous knowledge of the modulus of the construct, as prescribing too large a force may result in the fracture of sensitive, immature constructs. Our device measures both force and displacement, alleviating this potential complication. Additionally, as a construct evolves in terms of increasing modulus, the applied force would need to be continually adjusted to remain at a constant strain value. This demonstrates the advantage of simultaneous force and displacement feedback as opposed to only displacement.

Cost-saving measures were implemented throughout the device to limit expense resulting in an assembled cost estimated at 68% of published designs, that is a decrease of over 30%. Cost estimates were obtained by requesting quotations for the same or similar specification devices from manufacturers or distributors. The detailed breakdown of the component costs of the device described herein and of a published device is included as supplementary material

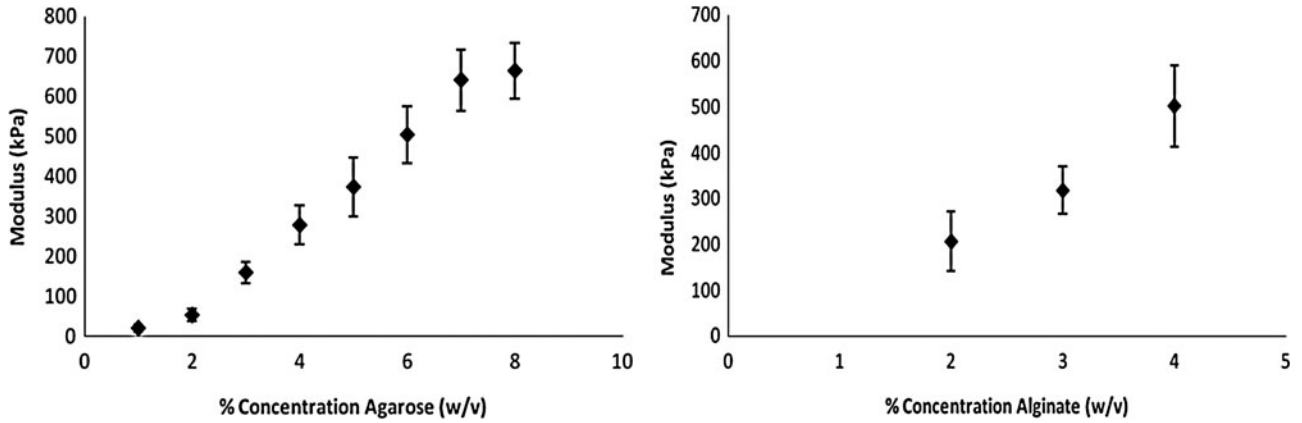

FIG. 5. Measured modulus values for increasing concentrations of agarose and alginate using our mechanical stimulator. Values are reported as an average ± standard deviation.

Table 2. Modulus Values for Materials Measured by Mechanical Stimulator

Material tested	*Modulus (kPa) (measured values)*	*Modulus (kPa) (literature values)*
2% alginate	206 ± 65	163 ± 9[15]
3% alginate	317 ± 51	302 ± 4[15]
4% alginate	501 ± 87	476 ± 11[15]
Biological material tested	*Modulus (MPa) (measured values)*	*Modulus (MPa) (literature values)*
Porcine cartilage	3.4 ± 0.6	2.6 ± 0.1[17]
Collagenase digested cartilage	1.5 ± 0.2	NA
Porcine cancellous bone	123 ± 27	37–167[19]

(Supplementary Tables S1 and S2). The cost savings arises primarily from decreased machining complexity. Only two components in the proposed design require more than precisely drilled holes. The selected linear actuator requires no motor amplifier, only a motor driver. The device lacks an expensive load cell for force sensing. Furthermore, long-term operating costs may be decreased by the use of standard tissue culture plastic, and the capability to measure modulus eliminates the need to purchase additional testing equipment.

The modular device design enhances its ability to be configured rapidly and inexpensively for numerous experimental parameters and samples. Components of the stimulation cassette are the only parts that should be altered to change construct size or stimulation type. To alter construct size, a new stimulation cassette appropriate for the repertoire of commercially available multi-well tissue culture plates can be rapidly exchanged. The new cassette would differ in layout and Teflon plunger diameter to correspond to the respective tissue culture plastic. Both these variables can be easily accommodated with the modular design (Fig. 1). Altering stimulation type requires simply exchanging the Teflon plungers for one of a different design. This is further discussed in the next section.

Finally, the software and broad operating specifications of the device allow for versatility in stimulation protocols. Stimulation parameters such as static offset or frequency may be rapidly changed by typing a new value in the user interface without the need for exchange of components. The force application range of the stimulator exceeds other designs allowing for the stimulation of materials as hard as cancellous bone, a feature not possible with other stimulators.

In summarizing the pros and cons of our design in comparison to those described in literature, it is worth highlighting five aspects of the current design (Table 3). Our force resolution of 12 mN represents a significant level of sensitivity. The contact error of 1.16% represents a true measure of variance independent of applied force. An important aspect enabling versatility in a stimulation device is the range of the platen. The range in our device is ~30× more than the Aufderheide design[10] and 7× more than the Lujan device.[14] In mimicking extreme rates of stress change, our device is a compromise between other designs. Finally, our design implements a linear encoder that is independent of sensing elements which reduces the complexity of further device enhancements.

Future design enhancements

The design of the device may be enhanced in two areas, force sensing range and plunger versatility. The sensing range of the device may be increased by implementing selectable feedback resistors into the op-amp circuits. Currently, the value of the resistor is fixed, which compels the user to relinquish some sensitivity in exchange for range. The current value of 499k ohms is more suited for high sensitivity than for

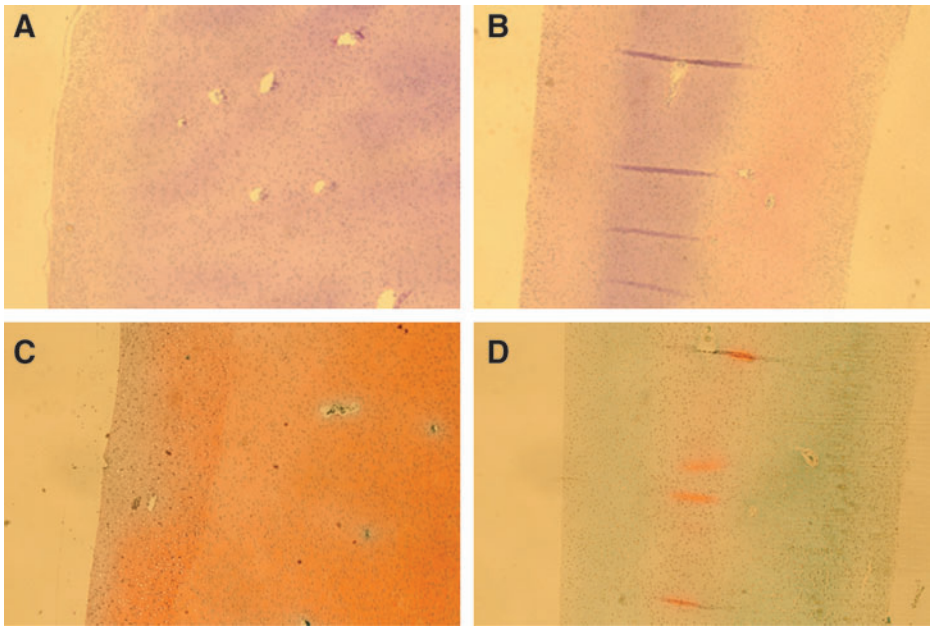

FIG. 6. Histological sections of native cartilage cultured for 12 h **(A** and **C)** and treated with collagenase for 12 h **(B** and **D)**. Tissue section was stained with Hematoxylin and Eosin **(A** and **B)** to visualize cell nuclei (black) and connective tissue (pink), and with Safranin O and Fast Green counterstain **(C** and **D)** to visualize proteoglycans (red).

Table 3. Specification Comparison Between Proposed Design and Three Others

	Proposed	*Aufderheide*[10]	*Demarteau*[11]	*Lujan*[14]
Estimated Cost	~$3500	~$6000	Not enough component information for estimate	Not enough component information for estimate
Individual sample force sensing	Yes	No	No	Yes
Force measurement	Resistance sensors	Load Cell	Load Cell	Electromagnetic actuators
Force Resolution	12 mN	NA	NA	NA
Simultaneous strain variation	Yes, different plunger material	No	No	Yes, actuators move independently
Simultaneous offset variation	Yes, different plunger height	No	Yes, move micrometer head	Yes, would require machining
Contact error %	1.16% ± 0.93%	NA	1.74% ± 0.36%	0% ± 10% @ 0.1 N
Position measurement	1 Linear Encoder	2 Linear Encoders	Na	Linear encoders integrated into each of 6 actuators
Max motor force	1200 N	445 N	NA	18 N peak, 10 N continuous
Platen range	101.6 mm	3 mm	NA	15mm
Tissue culture plastic compatible	Yes	No	No	Yes
Max speed	254 mm/s	30 mm/s	NA	1500 mm/s
Sample capacity	12	48	12	6

a large range of force values. The capability to change the sensitivity and range to suit a particular application would further enhance device functionality. For example, when a tissue construct is in the early development stages, a resistor value that offers high sensitivity may be chosen, and later substituted to enhance the range of force as the construct modulus increases. The device is currently implemented with 25-lb sensors. The same type of sensor is available in both 1-lb and 100-lb configurations. By tailoring the resistance of the op-amp circuits and altering sensor values, the range can be enhanced to better capture both low and high force values.

Long-term cultivation of constructs under various stimulation regimens needs to be carried out to optimize some of the design variables. We envision that the modular features and the low cost will allow for rapid evolution of the device to meet experimental needs. The device design anticipates implementation of many other stimulation modalities such as hydrostatic and shear stress; through alteration of the plunger configuration and material. The novel use of magnets to attach the plungers enables this rapid change. For example, to accommodate hydrostatic stimulation protocols, an O-ring may be placed around each plunger to ensure a seal between the plunger and the wall of the assay well, thus generating hydrostatic pressures. For shear stress stimulation, the plugs may be cut at a slight angle to impose lateral movement during the compression cycle, thereby producing shear stress in the construct. As an extension of fluid-induced stimulation, a system that simulates dynamic culture conditions by perfusion of culture media through a hollow plunger equipped with a fritted contact surface to enable fluid flow through the construct can be designed as well. Several studies have shown that electrical stimulation can positively impact synthesis of extracellular matrix components in cartilage constructs and bone tissue.[20,21] One can envisage the incorporation of a ring electrode on the plunger face, coupled with a plated well bottom for the application of electrical bias during mechanical stimulation. With regard to strain profiles, the height and modulus of the plunger can be varied to tune the offset strains and dynamic strain. The latter is a function of plunger stiffness. Plungers made of softer more deformable materials will absorb some of the load, thereby producing lower strains in the constructs.

Conclusions

We have proposed and validated a design of a mechanical stimulator that offers high-throughput, adaptability to standard tissue culture multi-well plates, functionality inside a standard incubator, and is capable of real-time modulus measurements which are accurate and sensitive, within a range that is relevant to the evaluation of *ex vivo* cartilage constructs. We have demonstrated that constructs with modulus as low as alginate gels and as high as cancellous bone can be determined without modification to the device design or components, thus increasing versatility. More importantly, the device is capable of discriminating between cartilage constructs differing in collagen composition, thus opening up the possibility of real-time mapping of changes to cartilage construct composition during mechanical stimulation. Due to the ease of configuration and adaptability, the device offers design solutions that increase experimental throughput to aid in the realization of functional *ex vivo* tissue constructs grown *de novo*.

Acknowledgments

This project was partially supported by a Discovery Grant from the Vanderbilt University to VPS. Support through the excellence intiative of the German Federal and State Governments grant EXC 294 is also acknowledged. The authors thank Ms. Isabel Syga for assistance with Supplementary Figure S2.

Disclosure Statement

The authors declare that they have no competing financial interests.

References

1. Blunk, T., Sieminski, A.L., Gooch, K.J., Courter, D.L., Hollander, A.P., Nahir, A.M., Langer, R., Vunjak-Novakovic, G.,

and Freed, L.E. Differential effects of growth factors on tissue-engineered cartilage. Tissue Eng **8,** 73, 2002.
2. Gooch, K.J., Blunk, T., Courter, D.L., Sieminski, A.L., Vunjak-Novakovic, G., and Freed, L.E. Bone morphogenetic proteins-2, −12, and −13 modulate *in vitro* development of engineered cartilage. Tissue Eng **8,** 591, 2002.
3. Gooch, K.J., Blunk, T., Courter, D.L., Sieminski, A.L., Bursac, P.M., Vunjak-Novakovic, G., and Freed, L.E. IGF-I and mechanical environment interact to modulate engineered cartilage development. Biochem Biophys Res Commun **286,** 909, 2001.
4. Darling, E.M., and Athanasiou, K.A. Biomechanical strategies for articular cartilage regeneration. Ann Biomed Eng **31,** 1114, 2003.
5. Grodzinsky, A.J., Levenston, M.E., Jin, M., and Frank, E.H. Cartilage tissue remodeling in response to mechanical forces. Annu Rev Biomed Eng **2,** 691, 2000.
6. Lee, C., Grad, S., and Wimmer, M.A. The influence of mechanical stimuli on articular cartilage tissue engineering. In: Ashammakhi, N., and Reis, R.I., eds. Topics in Tissue Engineering. Oulu, Finland: Expertissues, 2006, pp. 1–32.
7. Bonassar, L.J., Grodzinsky, A.J., Frank, E.H., Davila, S.G., Bhaktav, N.R., and Trippel, S.B. The effect of dynamic compression on the response of articular cartilage to insulin-like growth factor-I. J Orthop Res **19,** 11, 2001.
8. Darling, E.M., and Athanasiou, K.A. Articular cartilage bioreactors and bioprocesses. Tissue Eng **9,** 9, 2003.
9. Portner, R., Nagel-Heyer, S., Goepfert, C., Adamietz, P., and Meenen, N.M. Bioreactor design for tissue engineering. J Biosci Bioeng **100,** 235, 2005.
10. Aufderheide, A.C., and Athanasiou, K.A. A direct compression stimulator for articular cartilage and meniscal explants. Ann Biomed Eng **34,** 1463, 2006.
11. Demarteau, O., Jakob, M., Schafer, D., Heberer, M., and Martin, I. Development and validation of a bioreactor for physical stimulation of engineered cartilage. Biorheology **40,** 331, 2003.
12. Mauck, R.L., Soltz, M.A., Wang, C.C.B., Wong, D.D., Chao, P.H.G., Valhmu, W.B., Hung, C.T., and Ateshian, G.A. Functional tissue engineering of articular cartilage through dynamic loading of chondrocyte-seeded agarose gels. J Biomech Eng-Trans Asme **122,** 252, 2000.
13. Chen, H.C., and Hu, Y.C. Bioreactors for tissue engineering. Biotechnol Lett **28,** 1415, 2006.
14. Lujan, T.J., Wirtz, K.M., Bahney, C.S., Madey, S.M., Johnstone, B., and Bottlang, M. A novel bioreactor for the dynamic stimulation and mechanical evaluation of multiple tissue-engineered constructs. Tissue Eng Part C: Methods **17,** 367, 2011.
15. Stevens, M.M., Qanadilo, H.F., Langer, R., and Shastri, V.P. A rapid-curing alginate gel system: utility in periosteum-derived cartilage tissue engineering. Biomaterials **25,** 887, 2004.
16. Vunjak-Novakovic, G., and Freshney, R.I., eds. Culture of Cells for Tissue Engineering. New York: Wiley & Sons, 2006.
17. Stolz, M., Raiteri, R., Daniels, A.U., VanLandingham, M.R., Baschong, W., and Aebi, U. Dynamic elastic modulus of porcine articular cartilage determined at two different levels of tissue organization by indentation-type atomic force microscopy. Biophys J **86,** 3269, 2004.
18. Cowin, S.C., ed. Bone Mechanics Handbook. Boca Raton, Florida: CRC Press, 2001.
19. Mackenzie, J.K. Elastic constants of a solid containing spherical holes. Proc Phys Soc (London) **63B,** 2, 1950.
20. Gupta, R., Naranja, R.J., Levitz, C.I., and Brighton, C.T. The biochemical pathway of capacitively coupled electrical field stimulation of osteoblast-like cells. Proceedings of the 14th Annual Society for Physical Regulation in Biology and Medicine. New York: Society for Physical Regulation in Biology and Medicine. 1, 1994.
21. Korenstein, R., Somjen, D., Fischler, H., and Binderman, I. Capacitative pulsed electric-stimulation of bone-cells—induction of cyclic-AMP changes and DNA-synthesis. Biochim Biophys Acta **803,** 302, 1984.

Address correspondence to:
V. Prasad Shastri, Ph.D.
Institute for Macromolecular Chemistry
Hermann Staudinger Haus
Stefan-Meier Strasse 31
University of Freiburg
Freiburg D-79104
Germany

E-mail: prasad.shastri@makro.uni-freiburg.de;
prasad.shastri@gmail.com

Received: April 25, 2011
Accepted: October 10, 2011
Online Publication Date: December 29, 2011